IEEE International Conference on Robotics and Automation (ICRA), 2013

# A novel trocar-less, multi-point of view, magnetic actuated laparoscope

T. Ranzani, *Student Member, IEEE*, M. Silvestri, A. Argiolas, M. Vatteroni, A. Menciassi, *Member, IEEE*

***Abstract*— As a result of the rapid spreading of stereoscopy in the consumer market, three-dimensional (3D) vision systems are replacing two-dimensional devices. A fast growing technology in the 3D visualization systems market is multi-views autostereoscopic displays (ADs). However, these devices have not yet found a direct application in minimally invasive surgery (MIS), as it is really challenging to embed a high number of point-of-views in a device which has to pass through a MIS incision. The aim of this work is the development of a miniaturized vision acquisition system for MIS, which can be interfaced with multi-views ADs. The system is anchored by a magnetic link to the abdomen and freely moved by magnetic actuation to adjust the point of view and the horizon of the cameras. The laparoscope can embed up to 9 cameras, while matching typical MIS access incision size.**

## I. Introduction

One of the main concerns about Minimally Invasive Surgery (MIS) procedures, such as laparoscopy (traditional, and single port), is the loss of a direct view of the operative field. Standard laparoscopic imaging systems provide optimal performance in terms of image quality, details, and colour sharpness; however, several limitations are perceived by surgeons, first of all, the loss of depth perception, due to the two-dimensional (2D) visualization. In addition, they consist of rigid laparoscopes that fully take up one access port during the whole operation. Indeed, this scenario often leads to conflicts between the endoscopist manoeuvring the camera, and the surgeon controlling the assistive and operative instruments [1]. On the other hand, progresses in imaging system technologies have made three-dimensional (3D) view of the surgical field feasible and appealing, as demonstrated by the Da Vinci surgical robot [2] and by the Tricam imaging device [3]. However, these commercial devices use single-user 3D displays, while their acquisition systems still require a dedicated access port.

This last issue has brought research to focus on placing remotely controlled cameras entirely inside the abdomen, thus allowing more room at the incision site for additional tools and/or enhanced range of motion for existing tools [4, 5, 6]. Such devices can be inserted at the beginning of the intervention and fixed to the abdomen by suturing [4] or by exploiting a magnetic link between internally embedded permanent magnets (IPM) and external permanent magnets (EPM) [5, 6, 7, 8]. In this way, the access port is not taken up by the vision system during the surgical procedure. The use of magnetism can increase the manoeuvrability of the device by allowing a rapid repositioning of the system inside the abdomen. In addition the intra-abdominal magnetic link can be exploited for transmitting additional Degrees of Freedom (DoF) to an internal device, as demonstrated in [9].

Simi et al [10] explored the use of two-view autostereoscopic display (AD) in a magnetically held device, thus enabling 3D perception to more than one operator and avoiding the need of additional accessories. Although two-views ADs demonstrated their effectiveness in providing 3D cues of the surgical field [10], the current technology of multi-views ADs may further improve surgical performance by decreasing ocular fatigue, improving the 3D perception, and allowing the whole surgical staff to move in front of the display without losing any depth cue [11].

Currently, multi-views ADs have not yet found a direct application in MIS, mainly because of the encumbrance of the acquisition system: indeed, at least five aligned camera modules [12] must be embedded in a device that has to be inserted through the surgical incision. Aim of this work is the development of a multi-point of view acquisition system for MIS, which is able to fit the laparoscopic access incision.

The system is magnetically anchored to the abdomen, away from the incision port, and moved inside the abdomen thanks to completely passive 4-degrees of freedom (DoFs) actuation (Fig. 1). The number of point-of-views of the device will allow it to be interfaced with most of the commercially available multi-views ADs, thus paving the way to the use of such devices in surgery.

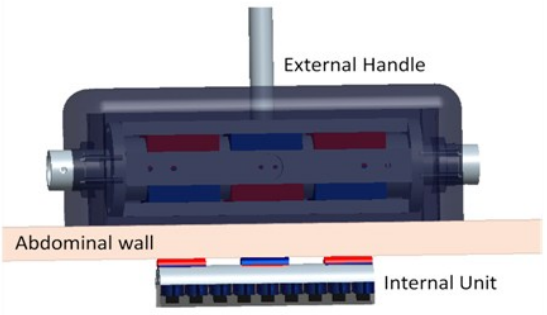


Fig. 1 Overview of the multi-point of view magnetic laparoscope.

This work was partially supported by the ARAKNES FP7 European Project no. 224565, the STIFF-FLOP FP7 European Project no. 287728, and the SUPCAM European FP7 Project no. 315378.

All authors are with The BioRobotics Institute, Scuola Superiore Sant'Anna, Pisa, Italy (email: n.surname@sssup.it).

T. Ranzani is the corresponding author (t.ranzani@sssup.it).

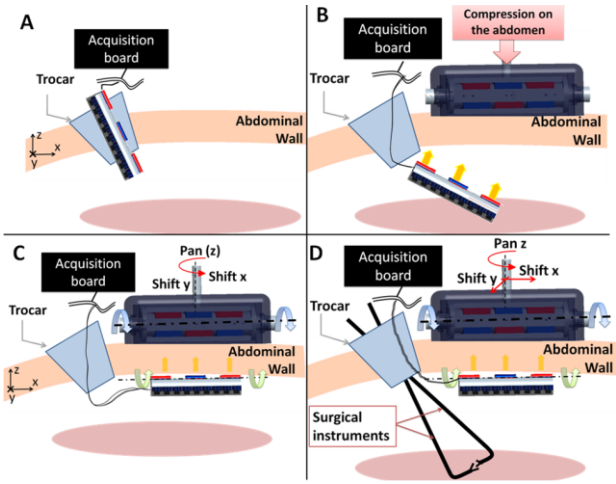


Fig. 2 Scheme of the different phases of use of the vision acquisition system.

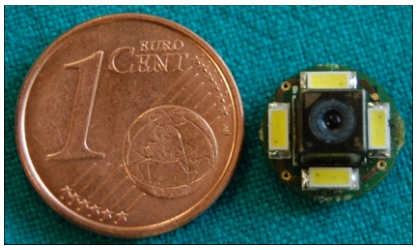

Fig. 3 The PCB (10 mm in diameter) embedding the CMOS camera and the lightning module.

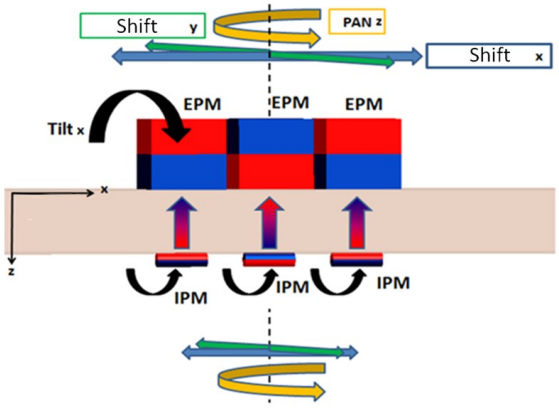


Fig. 4 Magnetic coupling and DoFs of the device

## II. Methods

One of the main issues in designing an acquisition system for multi-views ADs is the embedding of at least five aligned points of view [12] in a device with critical dimension requirements. A simple solution was found by the authors in the implementation of a module which can be inserted in the longitudinal direction, while anchored and manoeuvred in the horizontal one. Once inserted (Fig. 2 A), the vision acquisition system can be anchored to the abdominal wall (Fig. 2 B) and manually moved and positioned according to the surgeon requirements (Fig. 2 C). The possibility to position the vision acquisition system remotely from the insertion point allows to keep the trocar port free for the insertion of additional tools and surgical instruments as illustrated in Fig. 2 D. The presented device aligns the cameras within an internal unit, keeping constrained the overall dimensions and enabling an easy and quick positioning of the device on the internal abdominal wall. The device is based on an internal unit, for hosting and aligning properly up to 9 points of view (for complying with a major number of commercial multi-view ADs), magnetically linked to an external handle for anchoring, positioning, panning and tilting the vision acquisition system along the external surface of the abdomen.

### A. Vision Acquisition System Design

Commercially available multi-views ADs are not yet standard and require a highly variable number of acquisition points [12]. Considering MIS as the target application, authors identified a pool of suitable commercially available ADs by fixing the following set of specifications: a screen dimension ranging from 32" to 46", thus allowing a minimum viewing distance of 1.8 m, and a viewing angle as wider as possible in order to let most of the surgical staff to visualize properly the 3D display. The identified devices require a number of acquisition points varying from 5 to 9 [13, 14, 15]. Therefore, the authors decided to design the acquisition system as a modular camera combining a variable number of points of view and keeping the size of each of them as small as possible. The video acquisition system (Fig. 3) is based on a CMOS camera module (STMicroelectronics, Italy), 1616 × 1208 in resolution and 5 mm × 5 mm × 3.8 mm in size (Fig. 3). The imager is embedded on a Printed Circuit Board (PCB) of 10 mm in diameter, in order to meet the requirements that are declared by AD manufacturers [13, 14]. The PCB embeds also four white high efficiently Light Emitting Diodes (LEDs) for the illumination system. In order to keep the modularity of the device, LEDs are positioned around the camera in radial arrangement. Data transmission and power supply to a single camera module are ensured by a wired connection with an acquisition board which also allows visualizing and storing of the image stream on a laptop.

### B. Magnetic Link

The anchoring and magnetic orientation systems were designed in order to provide a simple control and an affective coupling of the internal unit with the external handle (Fig. 4). Besides the possibility to position the frame along the abdomen, the magnetic coupling is used for Pan and Tilt DoFs. The external unit is made by three off the shelf (KJ Magnetics, Jamison U.S.) cubic (30 mm x30 mm x 30 mm) permanent magnets (NdFeB, N52 magnetization grade) fixed on the handle and free to rotate around the *x* axis as in Fig. 4. Internally, three cylindrical (L = 20 mm, D = 6 mm) magnets (NdFeB, N52), are fixed on the internal frame corresponding to the external one. Panning and shifting of the internal device can be obtained by moving the external handle. The Tilt DoF is obtained exploiting the torque induced by the rotation of the external handle on the three magnets fixed in the internal unit. A 3D magnetic model was implemented using a Finite Elements Analysis (FEA) Software (COMSOL Multiphysics 3.5) to model the magnetic coupling between the external handle and the internal unit; since permanent magnets are used, magneto-

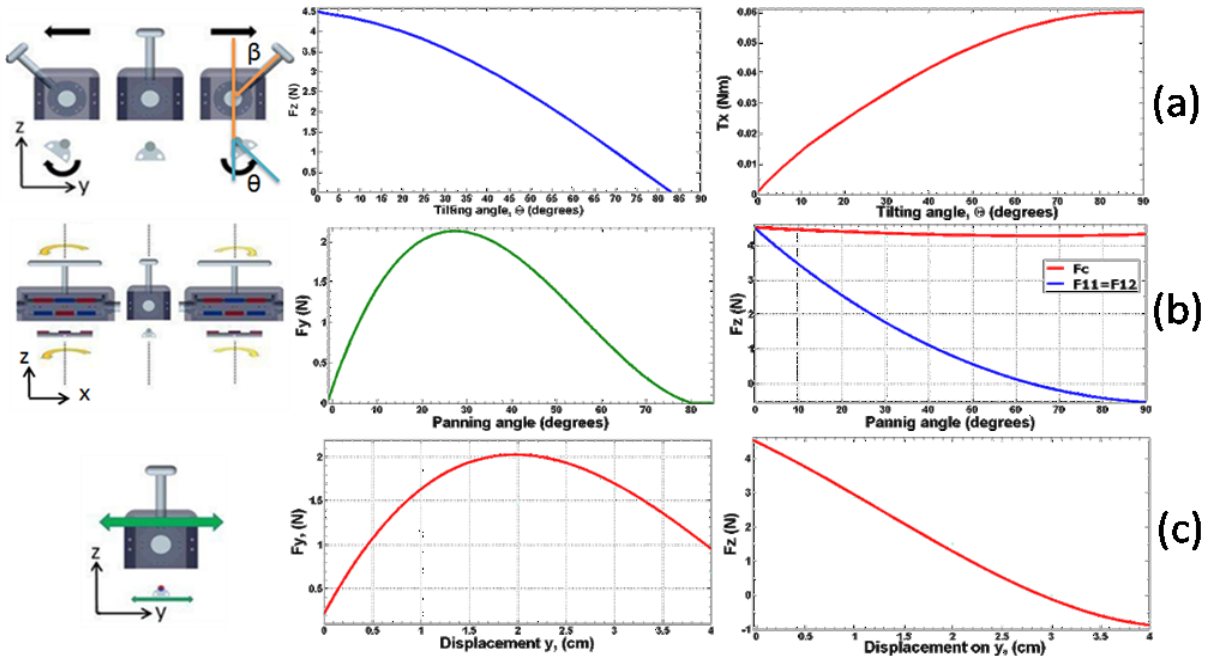


Fig. 5 Movements enabled by the magnetic coupling and computed forces; a) axial force and magnetically transmitted torque for the tilting DoF; b) forces involved in the panning (*Fy*, *Fz*). The *Fz* is computed on the central magnet ($F_c$) and on the lateral ones ($F_{l1}$, $F_{l2}$); c) forces involved in the shifting of the inner device (*Fy*, *Fz*).

static equation were implemented. The three cubic EPMs were positioned at a distance of 5 mm between each other and the IPMs were positioned aligned to the corresponding EPMs as illustrated in Fig. 4. The stability of the magnetic anchoring and the effectiveness of the magnetically transmitted DoFs were considered as the main constraints of the dimensioning process, while keeping the size of magnets within the Single Port Laparoscopy (SPL) incision limits. The model implements the following equations:

$$\begin{cases} -\nabla \cdot (\mu_0 \mu_r \nabla V_m - B_r) = 0 \\ B = \mu_0 \mu_r H + B_r \end{cases} \quad (1)$$

where $\mu_0$, $\mu_r$ are the vacuum magnetic permeability and the relative permeability, respectively. $B_r$ is the remanent flux density, H the auxiliary magnetic field and $V_m$ the magnetic potential. The remanent flux density was set to 1.465 T according to the magnets datasheets. For simulating the induced torque and the forces involved during the tilting of the EPMs on the IPMs the model was computed for different orientations of the magnetization of the EPMs, keeping fixed the IPMs one. The EPMs magnetization has been varied from 0° to 90°with a step of 1°. The simulation of the Pan DoF was performed by evaluating forces and torques induced at different Pan angles, in the range from 0° to 90°, with a step of 1°. Similarly the dragging of the internal unit was simulated computing magnetic forces when shifting the EPMs from the aligned position to a displacement of 4 cm (when the attraction force goes to zero) with a step of 1 mm. Results of the simulations are presented in Fig. 5. The anchoring force (*Fz*) was computed at 30 mm distance (corresponding to the typical abdomen thickness [16]) by rotating the magnetization of the EPMs and keeping fixed the IPMs one in order to consider how the attraction force varies in case of misalignment between the external handle and the internal unit. As shown in Fig. 5a the computed anchoring force is 4.5 N (when the EPMs and IPMs are aligned). In addition the internal device keeps anchored even if there is a 65° misalignment in the rotation. This value has been computed considering that the weight of the internal unit is 0.2 Kg (2 N). The computed torque induced has a maximum corresponding to the maximum misalignment between the internal and the external magnets and it reaches 0.06 Nm. Magnetic forces involved in the Pan DoF were simulated by rotating the internal unit along the *z* axis and fixing the position on the external handle, as shown in Fig 5b. The force along the *y* axis, which determines the realignment of the internal unit, grows up to 30° of misalignment, after that it decreases and the Pan motion is no more effective. However, as shown in the *Fz* graph of figure 5b, the attraction force of the central magnet is still enough to keep the device anchored. Finally, the magnetic forces generated in case of translation of the device were computed (Fig. 5c). The retraction magnetic force is effective up to 20 mm of misalignment, where it reached 2 N (corresponding to the internal device weight). However, as evident from the *Fz* graph in Fig. 5c, the anchoring force will not be able anymore to keep the device anchored after 15 mm in misalignment.

### *C. Mechanical Design*

The internal unit has the main function of hosting the various camera modules and keeping them stably fixed and aligned. As shown in Fig. 6 each camera is fixed to a structure that is inserted on a frame and aligned, correctly exploiting the grooves in the frame. On one side of this frame a glass slide is fixed, on the other the structure in Fig. 6 is used to block the cameras to the frame. The device is closed on the back by a semi cylindrical cap. This cap

hosts the three IPMs and guarantees the required space for managing the cabling. The external handle has a very simple design since its function consists in keeping the EPMs aligned and allowing the rotation of all of them around the axis parallel to the patient's abdomen (tilting).

## III. Experiments and Results

### A. Fabrication

The insertable unit and the external handle were designed and fabricated by rapid prototyping (Fig. 7 a, b) using a 3D Printer Invision Si2, Inition, with VisiJet XT 200 as acrilic photopolymer, and VisiJet S100 as support material. The insertable device fits in a boundary box of L x W x H = 73 mm x 17 mm x 21 mm, thus allowing it to be introduced from the incision performed during a single port laparoscopic procedure (which is about 20-30 mm). The dimensions of the external handle are L x W x H = 120 mm x 70 mm x 43 mm and the weight is 1.3 Kg thus exerting a pressure of $1.5 \times 10^{-3}$ MPa on the abdomen.

### B. Vision Acquisition System Assessment

One of the main constraints in designing a multi-views acquisition system was the correct vertical alignment of the cameras in order to avoid artifacts or ocular fatigue during the visualization. Therefore, the device was fixed on a support and images acquired by five cameras were stored (Fig. 8) and calibrated using Matlab™. The resulting alignment error was ±0.24°, which is less than the physiological limit (±0.32°), thus not introducing an uncomfortable vertical distortion [17].

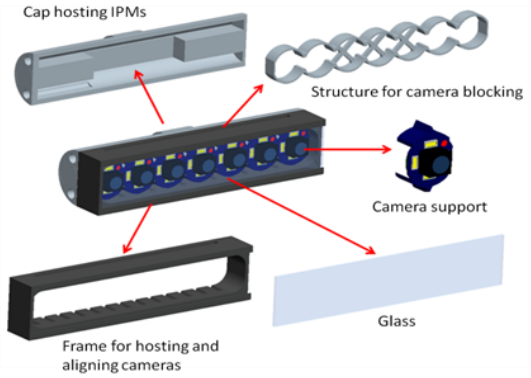


Fig. 6 Internal Unit: components overview.

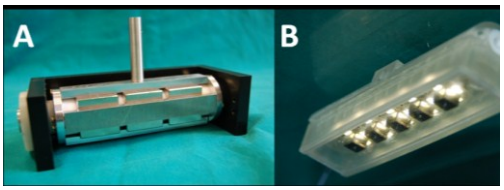


Fig. 7 External Handle (A), and internal unit (B).


Fig. 8 Images acquired for testing the alignment of the camera modules inside the internal unit.

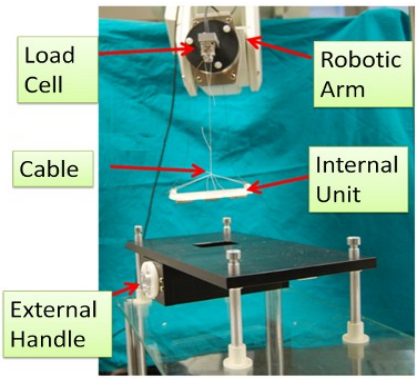


Fig. 9 Setup for the experimental evaluation of the anchoring force.

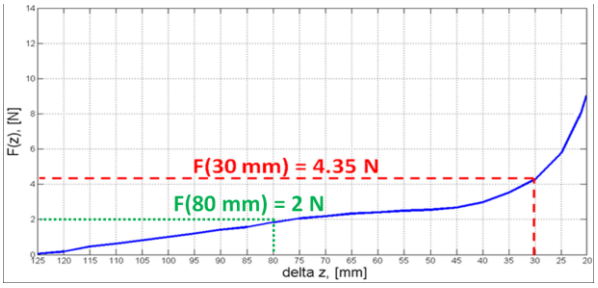


Fig. 10 Anchoring force as a function of distance.

### C. Magnetic Link Assessment

The variation of the attraction force with distance was validated by fixing the internal unit to an industrial robot (RV-6SL, Mitsubishi) and the external handle on a plastic plate. The measuring setup is shown in Fig. 9. Forces were measured by a 6 axes (NANO 17, ATI, USA) load cell fixed to the robot as shown in Fig. 9. The test was performed by moving the robotic arm along the $z$ axis with discrete steps equal to $\Delta z$ = 5 mm, from an initial distance of 15 mm, up to 125 mm. As described in Fig. 10, once inserted the internal unit inside the abdomen, it is sufficient to bring the external handle down to a distance of 80 mm from the internal magnets by compressing the abdominal wall, to generate the lifting of the internal device and the anchoring to the abdominal wall. Indeed, at 80 mm, the generated force balances the weight of the internal unit (i.e. 0.2 N). The force exerted by the internal unit on the abdominal wall is about 4.35 N at 30 mm of distance (i.e. the typical thickness of the abdomen wall), in agreement with simulations (tilting angle of the internal unit equal to 0) and with a 3% error.

Dynamic variations in the abdomen thickness due to oscillations of the pneumoperitoneum flow during laparoscopic procedures may lead to local abdomen thickness reduction, increasing the magnetic coupling and thus not affecting the functionalities of the device. In order to assess the absence of tissue injuries the pressure exerted on the abdominal wall at 9 mm thickness was computed as in [18]. In the case that only the three inner magnets are in contact with the abdominal wall, the surface is given by three times half of the lateral area of each magnet $3 * \left(2 * \pi \left(\frac{D}{2}\right) * L\right) = 565.49\ mm^2$; the computed anchoring force at 9 mm is 14.52 N thus generating a pressure of 3.71 psi onto the tissue that is below to the assessed value of 6.78 psi [18].

The torque induced by the external handle on the internal unit was experimentally evaluated by connecting the external handle to the robot in order to impose predefined rotations at discrete time intervals. The induced torque was derived by measuring the force transmitted through a rigid mechanical link between the outer lateral surface of the cap of the internal unit and the load cell, as shown in Fig. 11. The test consisted in rotating the external handle from 0° to 120°. The test was repeated 5 times and results showed a maximum error of 7% between the iterations. The choice of the range of values of β between 0° and 120° was dictated by the need to ensure the surgeon a wide range of tilting, without hazarding to break the magnetic link because of an excessive rotation of the handle.

The torque shows the same trend as obtained from the simulations as evident from Fig. 12 (top). The maximum experimental value of the torque is 0.06 Nm in accordance to the numeric simulations. It is important to emphasize that, unlike of the FEA analysis, in the case of experimental tests,

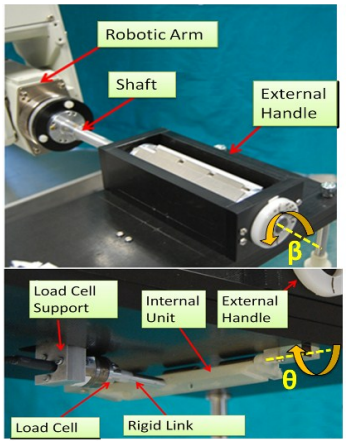


Fig. 11 Setup for the experimental evaluation of the transmitted torque.

the maximum torque is reached for values of 80°, instead of

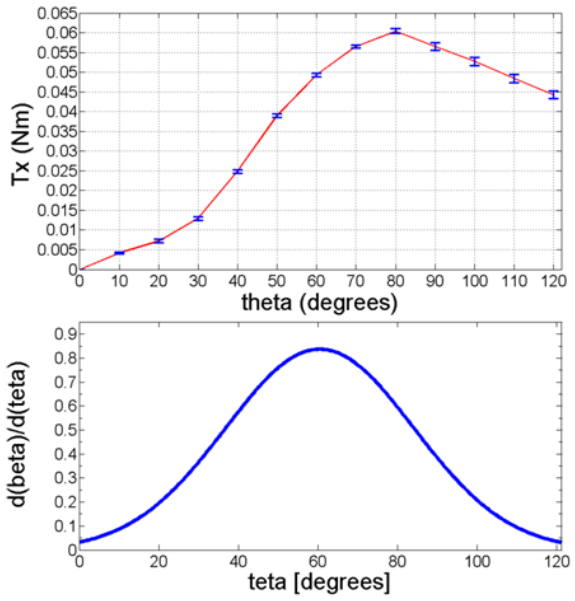


Fig. 12 Magnetically transmitted torque and angular resolution.

90° as resulting from the simulations (Fig. 5a). This difference is due to the friction between the magnets and the test plan, which was not taken into account during the simulation, and to possible misalignments that are caused by manufacturing tolerances.

The angular resolution of the internal unit rotation with respect to a corresponding rotation of the external handle was evaluated by measuring the tilting angle of the internal unit with respect to a robot-imposed rotation of the external handle ($\beta$). The tilting angle of the internal device ($\theta$) was evaluated using a camera: for each rotation imposed by the robot an image was acquired. The test was performed rotating the external handle from 0° to 120° with a fixed step of 5°. The tilting angle of the internal unit was evaluated using Matlab™. The derivative $\partial\beta/\partial\theta$ as a function of $\theta$ was evaluated and is presented in Fig. 12 (bottom). The graph shows that the response of the internal unit with respect to the rotation of the external handle presents a high efficiency for rotations up to 60°, in which the derivative $\partial\beta/\partial\theta$ assumes values close to 0.85. On the other hand, when the rotation angle is close to 0° and 120°, the rotations of EPMs are hardly perceived by IPMs, since the misalignment between the magnetic axes is not sufficient to induce a torque which is able of rotating the internal unit.

The experimental validation, however, has been provided for the characterization of the single degree of freedom of tilting. As regards dragging along the axes $x$ and $y$ and the panning around $z$, no additional validation was done besides the modeling, since the validation would involve the evaluation of the friction with the abdominal tissue, that could be hardly evaluated and that is beyond the scope of this paper.

### *D. Demonstrations*

The multi-point of view, magnetic actuated laparoscope has been successfully qualitatively tested into the abdomen of a human simulator, as illustrated in Fig. 13 and 14. The internal unit was introduced in the abdomen and by compressing the external handle over a flexible abdominal simulator the magnetic anchoring has been established. In

Fig. 13 Demonstration of tilting mechanism in a phantom test; on the top, external view; in the middle, view inside the abdomen of the internal unit; on the bottom, images acquired by one on-board camera.

Fig. 13 images captured during the tilting of the internal unit are reported while in Fig. 14 the panning is demonstrated. In both cases the view from outside (top), from inside the abdomen (middle) and from one on the on-board cameras are reported. The images from inside the abdomen where taken with a gastroscope while the ones from outside with a camera.

## IV. Conclusion

Although multi-views ADs present a lot of potential advantages in the MIS scenario, they still do not have a direct surgical application, mainly because of technical limitations. Indeed, it is difficult to integrate more than 5 points of view in a miniaturized device, which can be inserted through a MIS trocar. The presented system overcomes these problems by the integration of up to 9 camera modules inside a frame, which matches the laparoscopic access port dimensions.

Additionally, the magnetic coupling guarantees a stable anchoring and an easy manoeuvring of the device without interfering with the cameras functionality since the magnetic fields are static. The mechanical tests show reproducibility and accuracy in motion, while the external handle design guarantees an intuitive and user-friendly interface. Some preliminary demonstrations of the device have been reported. Finally, the modularity of the designed acquisition system allows the interface with a wide range of commercially available multi-views ADs.

Future work is related to the development of a custom interface which will enable the complete video stream acquisition to be visualized by a multi-views AD, thus enabling in-vivo applications of the device.

Fig. 14 Demonstration of PAN DoF in a phantom test; on the top, external view; in the middle, view inside the abdomen of the internal unit; on the bottom images acquired by one on-board camera.

## Acknowledgment

Authors would like to thank STMicroelectronics and Nichia for the components used in this work. Authors would like to thank Marco Salerno for the valuable support during the work and Dr. Gastone Ciuti for the contribution in the experimental tests.

## References

[1] P. Weibl, “Current Limitations and Perspectives in Single Port Surgery: Pros and Cons Laparo-Endoscopic Single-Site Surgery (LESS) for Renal Surgery”, *Diagn and Ther Endosc*, 2010 (2010), ID 759431.

[2] J. H. Kaouk et al., “Robotic single-port transumbilical surgery in humans: initial report”, *BJU international*, vol. 103, pp. 366 – 369, 2008.

[3] KarlStorz website: http://www.karlstorz.com/.

[4] T. Hu et al, “Insertable Stereoscopic 3D Surgical Imaging Device with Pan and Tilt”, in *Proceedings of the 2nd Biennial IEEE/RAS-EMBS*, Scottsdale, AZ, USA, October 19-22, 2008.

[5] J. Cadeddu et al, “Novel magnetically guided intra-abdominal camera to facilitate laparoendoscopic single-site surgery initial human experience”, *Surg Endosc*, vol 23, pp. 1894-1899, 2009.

[6] M. Simi et al, "Magnetic Levitation camera robot for endoscopic surgery," IEEE *International Conference on Robotics and Automation (ICRA), 2011* pp.5279-5284, 9-13 May 2011

[7] M. Fakhry et al., “Visual exposure using single-handed magnet-driven intra-abdominal wireless camera in minimal access surgery” Surgical Endoscopy, Springer-Verlag, 2009, 23, 539-543

[8] B.S. Terry et al., "Single-Port-Access Surgery with a Novel Magnet Camera System," Biomedical Engineering, IEEE Transactions on , vol.59, no.4, pp.1187-1193, April 2012

[9] C. Di Natali et al., "Trans-abdominal Active Magnetic Linkage for robotic surgery: Concept definition and model assessment," IEEE International Conference on Robotics and Automation (ICRA), 2012, pp.695-700, 14-18 May 2012

[10] M. Simi et al, “Magnetically Activated Stereoscopic Vision System for Laparoendoscopic Single Site Surgery”, IEEE T Mech, *Published on line*

[11] M. Silvestri et al, “Autostereoscopic Three-Dimensional Viewer Evaluation Through Comparison with Conventional Interfaces in Laparoscopic Surgery”, *Surg Innovation*, vol. 18, pp. 223–230, 2011.

[12] H. Urey et al, “State of the Art in Stereoscopic and Autostereoscopic Displays”, in *Proc IEEE*, vol. 99, n. 4, pp. 540–555, 2011.

[13] Tridelity website, available at: http://www.tridelity.de. Last access 28/01/2013.

[14] Alioscopy website, available at: http:// www.alioscopy.com. Last access 28/01/2013.

[15] Magnetic 3D website, available at: http://www.magnetic3d.com. Last Access 28/01/2013/.

[16] C. Song, et al., “Mechanical properties of the human abdominal wall measured in vivo during insufflation for laparoscopic surgery”, Surgical Endoscopy, 2006; Vol. 20, pp. 987-990.

[17] Y. J. Jung et al., “Visual comfort assessment metric based on salient object motion information in stereoscopic video”, J Electron Imaging, vol. 21, n. 1, pp. 011008-1- 011008-16, Feb. 2012.

[18] L. Sara et al, “Magnetic Anchoring and Guidance System Instrumentation for Laparo-endoscopic Single-site Surgery/Natural Orifice Transluminal Endoscopic Surgery: Lack of Histologic Damage After Prolonged Magnetic Coupling Across the Abdominal Wall”, Urology, vol. 77, pp. 243-247, 2011.